

# Plastic Design of Biaxially Loaded Beam-Columns

B. C. RINGO, J. F. McDONOUGH, and T. M. BASEHEART

IN THE FIELD of engineering design, it is normal to design steel wide-flange columns as if they were loaded by direct compression or by a thrust with some eccentricity about only one of the principal axes. Only limited design information is available concerning the case where there exists, simultaneously, some eccentricity with respect to each of the major axes. Where careful consideration is given to the true loading on a wide-flange column, it is frequently found that the longitudinal thrust on most columns does have some eccentricity in both principal directions. Figure 1 illustrates this general loading situation.

The AISC Specification<sup>1</sup> contains plastic design rules for axially loaded wide-flange columns with either no moment or with moment about only one principal axis. The design criteria for the ultimate load-carrying capacity of a biaxially loaded beam-column is obtained by an implied extension of Formulas (2.4-2) and (2.4-3). It has, therefore, been desirable for some time not only to predict the ultimate load-carrying capacity of a member loaded in this manner, but to provide additional design criteria for the selection of such members.

This paper presents a design technique for determination of the maximum plastic strength of biaxially loaded beam-columns. The loading situation is caused by a compressive force eccentric to each of the two principal axes. The eccentricities are not restricted in any way. The member is an open section, composed of prismatic elements, of the wide-flange class, in which no stress reversals occur. The material is assumed to be ideally elastic-perfectly plastic, but may contain residual stresses. The analytical procedure used to determine the ultimate load is based on an equilibrium technique in which the external forces acting on the cross section are equated to the internal resistances of that section as determined

by the distribution of longitudinal stresses. The procedure is iterative and non-incremental. The principles of the procedure are presented in this paper as well as the results in the form of an interaction curve, design charts, and the equations of forces as used in the analytical procedure.

## EQUILIBRIUM APPROACH

The non-incremental equilibrium approach was first presented with respect to biaxially-loaded beam-columns by Ringo<sup>16</sup> in 1964 and later refined and extended by McDonough<sup>14</sup> in their doctoral dissertations. The approach applies to wide-flange members normally considered to be column sections in the AISC Specification.<sup>1</sup> The equilibrium approach derives its name from the fact that the solutions are obtained by equating the internal forces, both the compressive force and the moments, to the external forces acting on the cross section.

When given bending moments, as defined by a compressive load and its eccentricities, act on a beam-column, the column with "length" will have less capacity for load than the same column section when it is

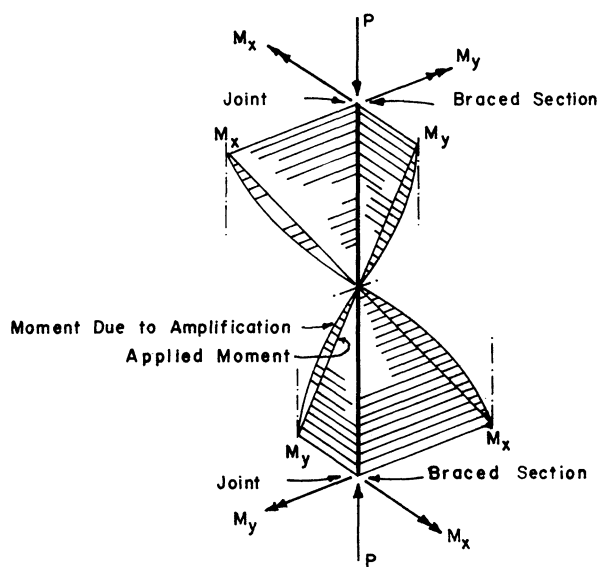


Fig. 1. Distribution of moments

B. C. Ringo is Professor of Civil Engineering, University of Cincinnati, Cincinnati, Ohio.

J. F. McDonough is Asst. Professor of Civil Engineering, University of Cincinnati, Cincinnati, Ohio.

T. M. Baseheart is Instructor of Civil Engineering, University of Cincinnati, Cincinnati, Ohio.

fully braced. It has, therefore, been customary to provide two equations for design purposes. One applies to the entire member and includes the effects of length. The other applies to cross sections or members whose effects of length have been prevented or are otherwise negligible. It is to the latter case that the method of this paper applies; that is, to the fully braced section. Because lateral-torsional instability is prevented at the cross section which is fully braced, each fiber of the section may be longitudinally stressed to its yield point before the ability of the cross section to absorb loading has been exhausted. Figure 2 illustrates the distribution of moments appropriate to this situation.

It is for this particular loading configuration that the AISC adopted a formula to cover this problem in the uniaxial situation. It is Formula (2.4-3), which gives the maximum strength of a beam-column subjected to a compressive thrust eccentric from one principal axis only. This equation is:

$$\frac{P}{P_y} + \frac{M}{1.18M_p} \leq 1.0$$

where  $M < M_p$ . This interaction equation applies to one of two possible cases of beam-column behavior. The member is fully braced as defined by the limitations placed on the value of  $(l/r)_{max}$  in Sect. 2.9, or the member may be under the action of forces which place it in double curvature. In the latter case, the critical forces and the formation of the plastic hinge, or its equivalent  $M_{pe}$ , occur at the ends of the member, rather than within its length. This paper extends the design capability to biaxial moment and applies to the same general situation as does AISC Formula (2.4-3).

The internal forces of resistance are first determined by a set of equilibrium equations. These equations are determined by sequentially setting positions of the neutral axis and, at the same time, assuming it to be a

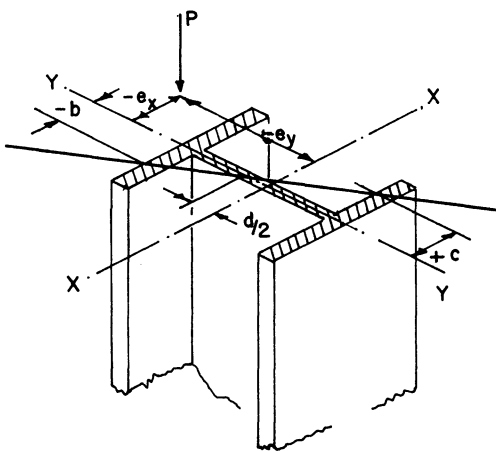


Fig. 2. Cross section and loading

straight line. Such is not categorically the case, but the error thus created is negligible, as has been indicated elsewhere.<sup>4</sup> The position of the neutral axis defines those areas on the surface of the cross section whose fiber stresses are in tension and those areas in compression. By assuming moments of these forces with respect to the principal axes, and by summing the longitudinal forces, the two moments and the compressive thrust are defined internally. Since the internal capacity must be equal to the externally applied forces, the maximum external load and its limiting eccentricities are readily, but not easily, computed. By studying each wide-flange column of interest in a like manner, and by making use of the appropriate characteristics of the high-speed digital computer, the complete domain of solutions has been established in table form for all beam-columns of interest.<sup>2</sup> One may then develop a family of interaction curves for each cross-sectional member. This has been done, and seven such families of curves are shown in Figs. 5 through 11, later in this paper. It is to be noted that the values on the charts are stated in absolute values rather than in non-dimensional ratios. This facilitates the design process.

To avoid complication caused by the interaction of the member and the frame of which it is a part, the scope of this work has been limited to the same degree as has been done by other investigators.<sup>9,18,15</sup> However, it is no more limited than are the AISC formulas previously mentioned. Following are the limitations and assumptions of significance to the design charts developed and illustrated in this paper:

1. The member is prismatic and of the wide-flange family.
2. The stress-strain curve is conventionally bi-linear.
3. It is assumed that strain hardening does not occur and that no fiber prematurely ruptures.
4. The thrust and the moments are continually increasing, and their rates of change with respect to deformations of the cross section are non-zero until the ultimate load has been achieved.
5. The geometry of the cross section is not altered by loading.
6. No account of the rate of application of load is included.

## EQUATIONS

The principles of the equilibrium approach will be briefly discussed here and the basic equations will be stated. The complete discussions and derivations are available in the work of McDonough.<sup>14</sup> The notation for the cross-sectional properties, where these sections are prismatic and of the wide-flange class, is defined in Appendix A. Other parameters of interest are defined in Appendix B. The notation related to the cross-sectional

geometry is graphically depicted in Fig. 3, which also shows dimension  $b$  as it is used to position the neutral axis on the cross section of the tension flange (dimension  $c$  at the compression flange is similar), and thus define the required forces. From the geometry shown in Fig. 3, one additional parameter used in the equation is  $d$ , where

$$d = d_{wf} \left[ \frac{1 + (b/c)}{1 - (b/c)} \right] \quad (1)$$

The basic equations for moment and longitudinal thrust as derived are:

$$P = F_y t_w d + 2t_f(c + b) \quad (2)$$

$$M^x = F_y t_f d_{wf}(c - b) + \frac{1}{4} t_w (d_{wf} - t_f)^2 - d^2 \quad (3)$$

$$M^y = F_y t_f (\frac{1}{2} b_f^2 - c^2 - b^2) \quad (4)$$

where  $d \leq d_{wf}$ ,  $c \leq \frac{1}{2} b_f$ , and  $b \leq \frac{1}{2} b_f$ .

By the selection of the values of  $b$  and  $c$ , the neutral axis is positioned and a particular solution is established. However, as these equations are stated, they cannot account for the variations in force across the widths of elements, nor can they account for situations in which the neutral axis intersects only the flange, or only one flange and the web. These are special cases as far as the equations are concerned, and when they do occur there must be correction terms added to the equations above. There are fourteen such special situations, not all of which exist simultaneously. The resulting equation of moments with the appropriate correction terms and the corresponding equation for longitudinal thrust  $P$  are extremely complicated, inasmuch as there are a considerable number of terms and an involved logic used to select the appropriate terms in each equation. For all options, the corresponding correction terms appear in Ref. 14 and will not be repeated in their entirety. As an illustration, however, the correction equation for a particular case of  $M^x$  is stated here as Eq. (5), as dictated by the situation shown in Fig. 4, which illustrates the position for a large magnitude of thrust ( $P$ ), a small magnitude of major axis moment ( $M^x$ ), and negligible value of minor axis moment ( $M^y$ ). The appropriate correction to the magnitude of  $M^x$  is:

$$dM^x = \left( \frac{d}{c - b} \right)^2 t_w^2 t_f F_y + 2 \frac{(c - b)}{d} t_f^3 F_y + \left[ \frac{t_f(c - b)}{2} + b - \frac{b_f}{2} \right]^2 \left[ \frac{(d - t_f)}{2} + \frac{t_f(c - b)}{2d} + b - \frac{b_f}{2} \right] \frac{d^2}{3} F_y - \left[ \frac{t_f(c - b)}{2} - b - \frac{b_f}{2} \right]^2 \times \left[ \frac{d - t_f}{2} + \frac{t_f(c - b)}{2} - b - \frac{b_f}{2} \right] \frac{d^2}{3} F_y \quad (5)$$

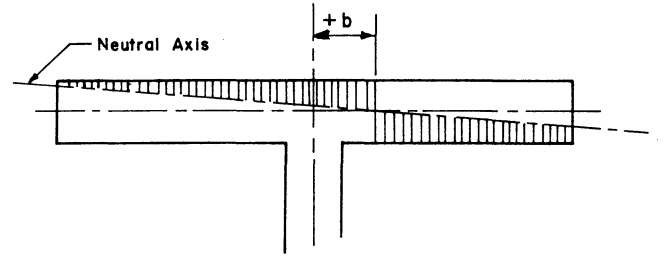


Fig. 3. Neutral axis on section

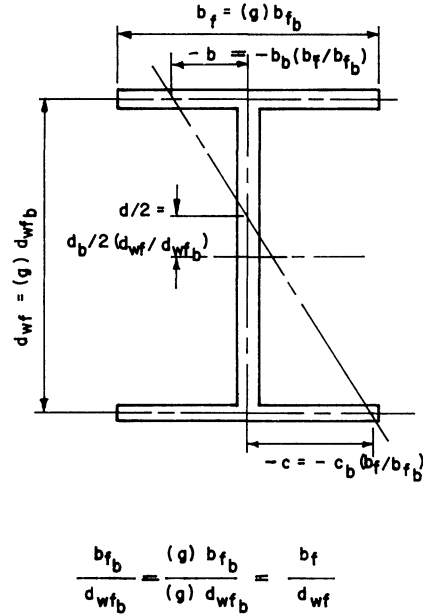


Fig. 4. Proportioning neutral axis positions in cross sections

The final equation for a particular situation (position of the neutral axis corresponding to a thrust with two eccentricities) required to give the maximum moment is the sum of Eqs. (3) and (5).

Each wide-flange cross section of interest was investigated by varying the values of  $b$  and  $c$  in these equations and, in turn, providing an output of combinations of  $M$ ,  $M^x$ , and  $M^y$  for each particular member. This provided the raw data from which the interaction curves and the design graphs were developed.

#### PROPORTIONALITY CONSTANTS

In the previous material, the ultimate compressive loads and their corresponding biaxial moment capacities for various members have been established. It is not impossible to use a single chart or a somewhat more comprehensive set of graphs for each cross-sectional shape for design purposes; however, the number of charts or graphs would indeed be cumbersome. For the column sections

selected, 73 such graphs would be a minimum for accurate results.<sup>2</sup> In order to reduce the volume of design aids required, and in order to make the design process more tractable, Baseheart has established a relationship between sets of selected members and their most representative section, called the base section. This relationship is, in fact, a dimensionless geometrical constant. It allows the relationships between forces (longitudinal thrust and biaxial moments) on a particular cross section, called the base section, and similar forces on other wide-flange sections in the same group to be established. The groups are formed to effect an acceptable compromise between exactness and tractability of design. The geometrical relationships are briefly presented in this part of the paper.

Figure 4 shows the basis for the derivation of the geometrical constant when the ratios of  $b_f$  to  $d_{wf}$  are approximately the same. The position of the neutral axis is set to the same relative position on all cross sections; thus, the values of  $b$  and  $c$  are set proportional to the widths of the members' respective flanges. The forces that are the internal capacities of these sections are then also similarly proportioned. However, as no two wide-flange sections are exactly proportional in this manner, base sections are selected such that, for sections in their group, the arithmetic discrepancies inherent in this method result in final design selections that are within 5% of an exact numerical solution.<sup>2</sup>

The following relationships can be obtained by substitution and by dividing the load capacity of the base section by the load capacity of any other section in that group:

$$P_b = \left(\frac{t_{fb}}{t_f}\right)\left(\frac{b_{fb}}{b_f}\right)P = R_1P \quad (6)$$

$$M_{x_b} = \left(\frac{t_{fb}}{t_f}\right)\left(\frac{d_{wfb}}{d_{wf}}\right)\left(\frac{b_{fb}}{b_f}\right)M^x = R_2M^x \quad (7)$$

$$M_{y_b} = \left(\frac{t_{fb}}{t_f}\right)\left(\frac{b_{fb}}{b_f}\right)^2M^y = r_3M^y \quad (8)$$

In these equations  $R_1$ ,  $R_2$ , and  $R_3$  are the geometrical constants which define the relationships between the thrusts and moments on the base sections and all other sections of its groupings for proportional locations of the neutral axis. The significance of these expressions is that they allow one interaction graph, with a family of  $P$  curves, to be used for the analysis of all cross sections in a particular grouping of members. These groupings, seven in number, for the 73 columns selected, were developed by a computer search.

#### DESIGN GROUPS

Once the family of interaction curves for the base section have been developed, and the interaction force values for the other wide-flange sections in each grouping

have been established such that they are proportional to that group's base section, the multiplicity of moment and load combinations can be plotted. This set of moments and loads, which corresponds to any particular position of the neutral axis, and which defines the permissible domain of  $P$ ,  $M^x$ , and  $M^y$ , can be set up as a convenient design chart. Such charts (Figs. 5–11) are readily usable for direct design by practicing engineers. Were it not for the grouping of sections in terms of one base section, there would have to be one interaction graph for each cross-section, instead of seven design nomographs, one for each group.

For example, Fig. 5 (upper right) shows the family of interaction curves for the base section of group 1, which is a W14×95 member. Figure 5 also shows the straight lines relating the various other sections of the grouping to the base section through the use of  $R_2$  (in the case of  $M^x$ ) and  $R_3$  (in the case of  $M^y$ ). An illustrative example shows how one uses the graphs to relate the values of  $M^x$  and  $M^y$  and the corresponding ultimate load  $P$  for a given section.

The interaction forces for the base sections are determined directly from the upper right-hand graph in Fig. 5, but for other sections in this grouping, forces are proportioned to the base section values by means of the constants  $R_1$ ,  $R_2$ , and  $R_3$ . Since the values  $R_2$  and  $R_3$  which define this relationship are dimensionless constants, the lower right and upper left graphs in Fig. 5 automatically establish the relationships of Eqs. (7) and (8). This is done by making the slope of the straight lines, for other sections of the group, equal to  $R_2$  times the slope of the straight line for the base section. The same process follows for  $R_3$ . The base section thrust can be obtained from the interaction of the moment values in the upper right-hand graph of Fig. 5. The thrust  $P$  for any cross section in the grouping can then be calculated using Eq. (6) and the  $P_b$  value read from the graph. Thus, design is handled by the three graphs combined into a nomograph. One such nomograph is used for each of the seven member groupings.

#### NUMERICAL EXAMPLE

An example problem is shown illustrating the use of the base section interaction graphs, i.e., the nomograph, for determining the maximum load for a wide-flange section which is subjected to moments about each of the two principal axes.

*Given:* Applied  $M^x = 1705.0$  kip-in.

Applied  $M^y = 325.3$  kip-in.

Selecting a W10×54 column section of ASTM A36 steel ( $F_y = 36.0$  ksi), find the maximum compressive thrust,  $P$ .

From Appendix B, the W10×54 is a member of Group 1, in which the W14×95 shown in Fig. 5 is the





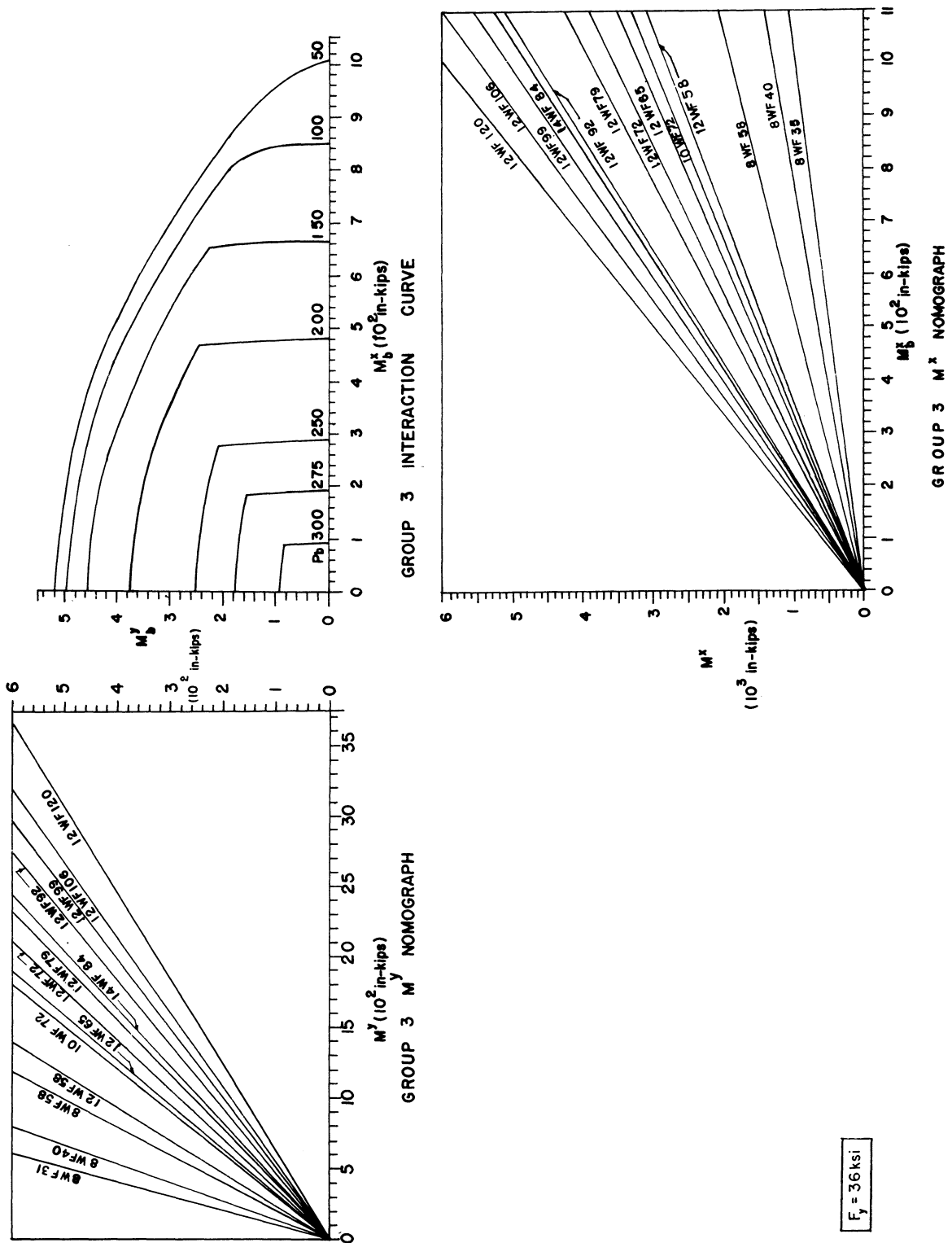
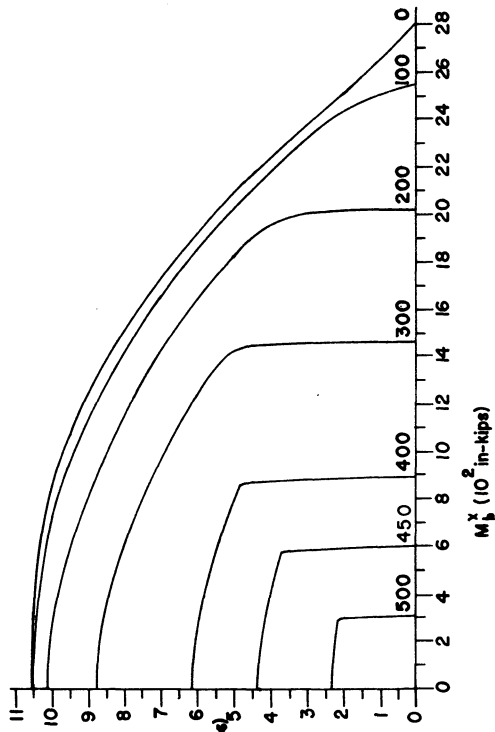
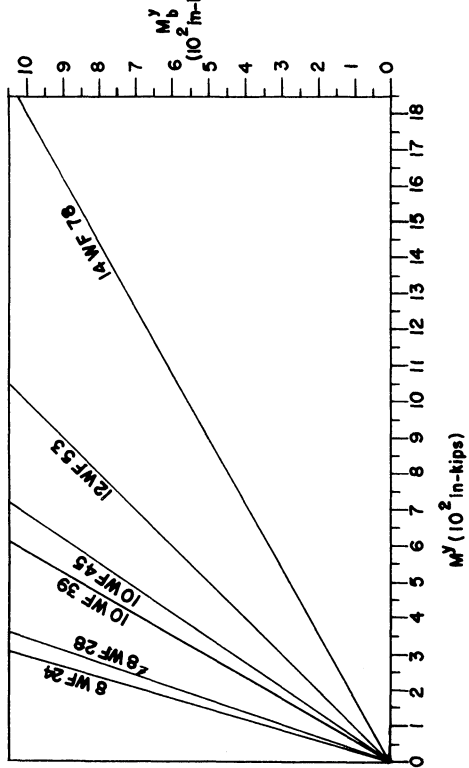
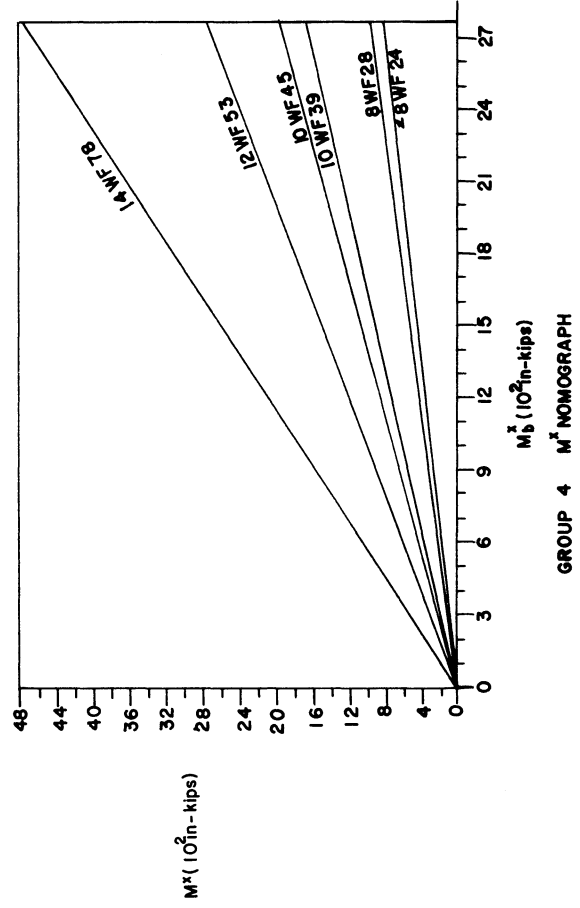


Fig. 7. Interaction curves and nomographs: Group 3



GROUP 4 INTERACTION CURVE



GROUP 4  $M_y M_x$  NOMOGRAPH

$F_y = 36 \text{ ksi}$

Fig. 8. Interaction curves and nomographs: Group 4



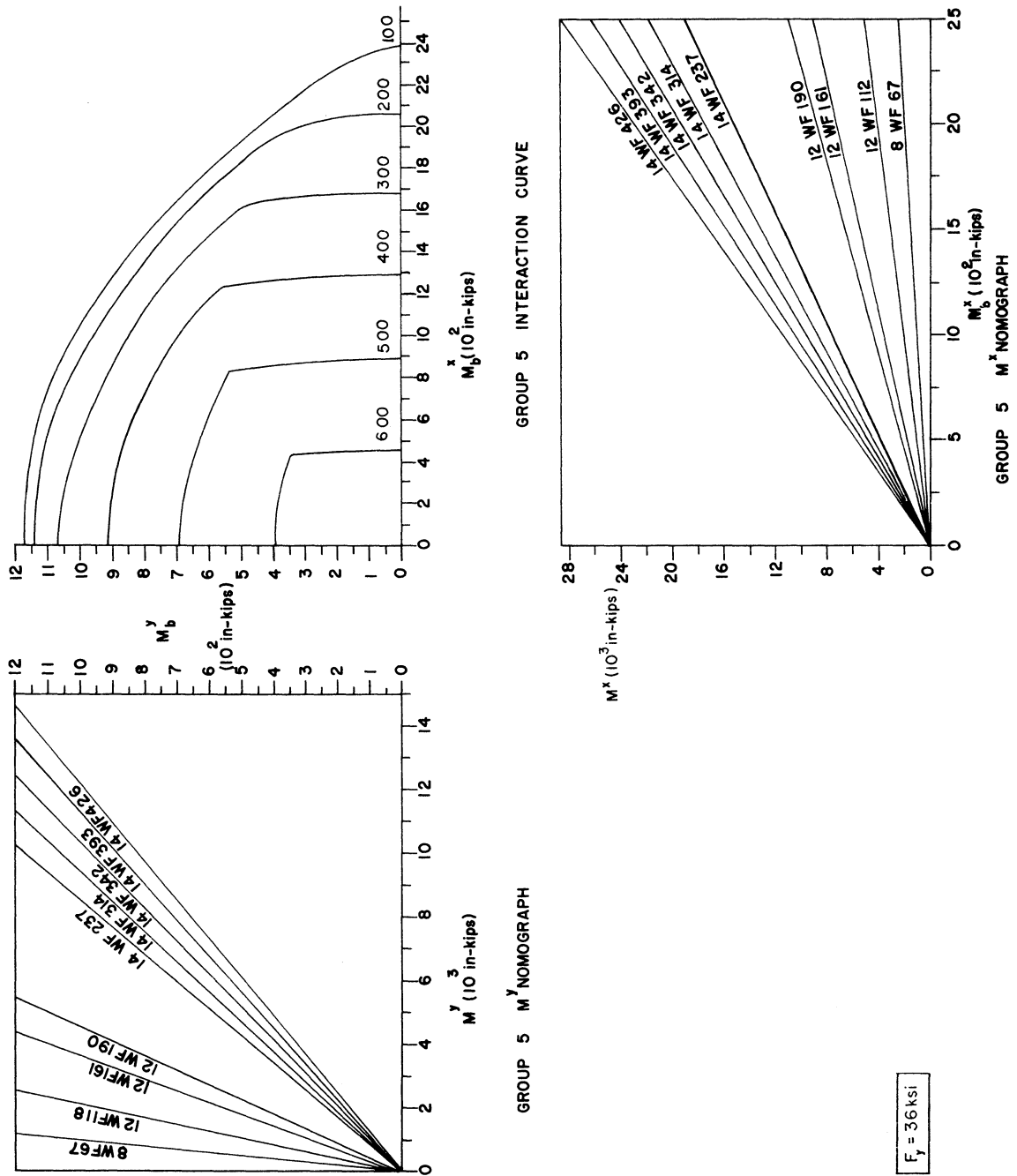
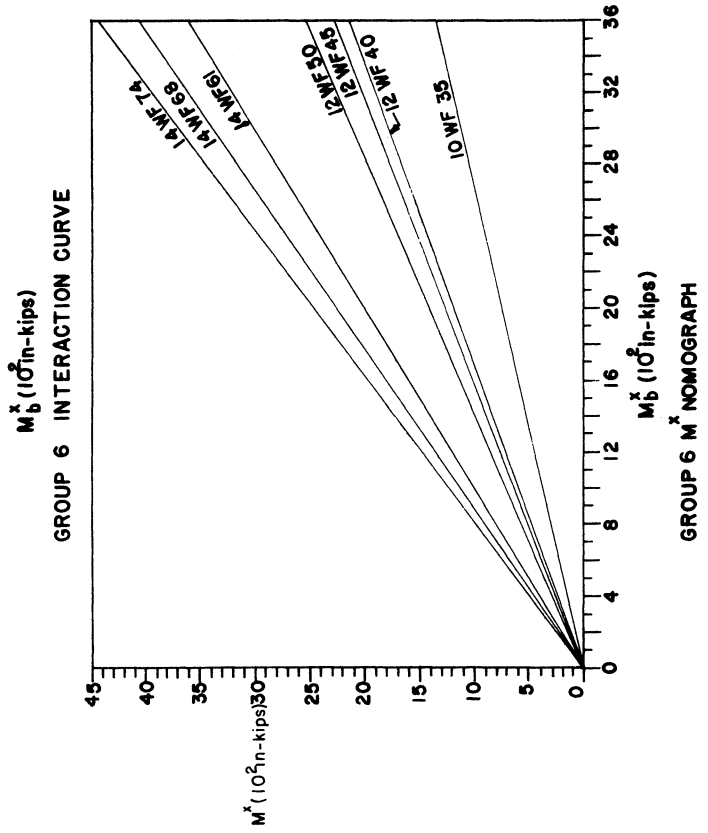
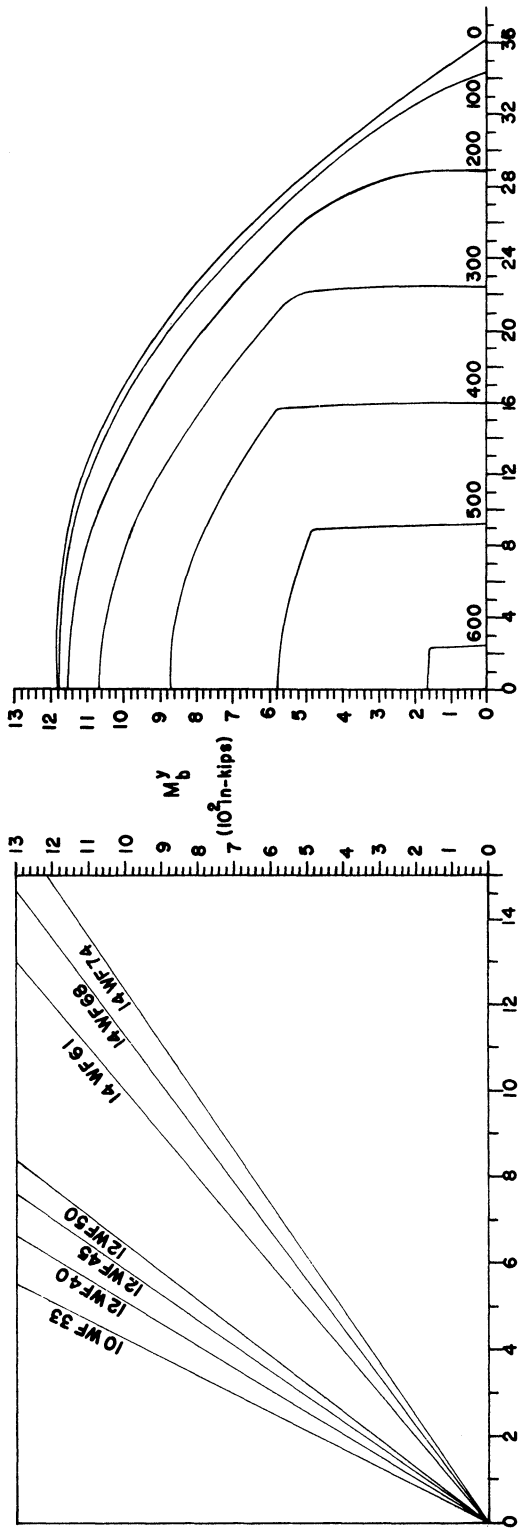
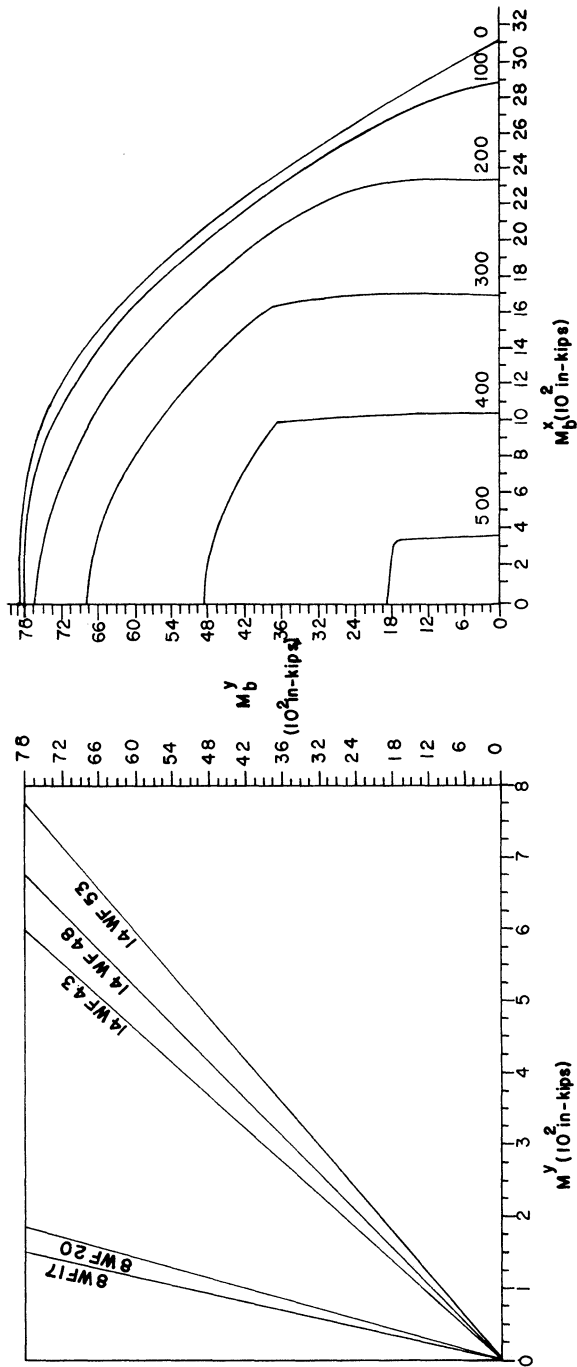


Fig. 9. Interaction curves and nomographs: Group 5

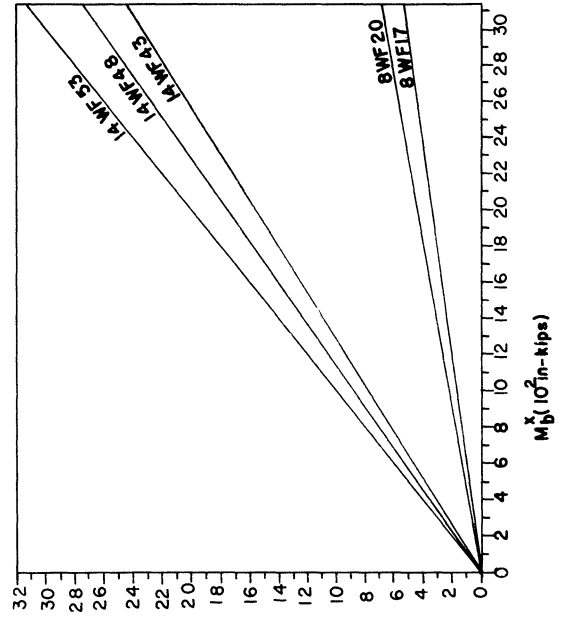


$F_y = 36 \text{ ksi}$

Fig. 10. Interaction curves and nomographs: Group 6



GROUP 7 INTERACTION CURVE



GROUP 7  $M^x$  NOMOGRAPH

$F_y = 36 \text{ ksi}$

Fig. 11. Interaction curves and nomographs: Group 7

base section and has a load capacity  $P_b = 365$  kips. This is determined from the equivalent  $M_b^x$  and  $M_b^y$  values, both of which may be determined graphically as indicated on Fig. 5. From Appendix B, one obtains  $1/R_1 = 0.570$  for the W10×54. Therefore, from Eq. (6), the following is computed:

$$P = (1/R_1)P_b = (0.570)(365) \\ = 208 \text{ kips}$$

This semi-graphical procedure gives a value of 208 kips of longitudinal thrust as the limiting loading when the given moments exist on the braced cross section. An exact numerical solution for the same loading case gives as  $P$  a value of 207.1 kips.<sup>14</sup>

### CONCLUSION

This paper has presented a design procedure from which one can readily calculate the maximum compressive load that a column can accept while subjected simultaneously to bending moments about both of the principal axes. Although a precise percentage of error for any given solution from the graphs is not mathematically derivable, the authors have used a numerical process to determine that the error from this design process is less than 5 percent. The intent of Part 2 of the AISC Specification has therefore been extended by a conservative and simple design procedure.

### REFERENCES

1. Specification for the Design, Fabrication and Erection of Structural Steel for Buildings *American Institute of Steel Construction, February, 1969.*
2. Baseheart, T. M. Design Graphs for Biaxially Loaded Beam-Columns *M. S. Thesis, University of Cincinnati, 1969.*
3. Birnstiel, C. Experiments on H-Columns under Biaxial Bending *Journal of the Structural Division, ASCE, Vol. 94, No. ST10, October 1968, pp. 2429-2449.*
4. Birnstiel, C. and Michalos, J. Ultimate Load of H-Columns under Biaxial Bending *Journal of the Structural Division, ASCE, Vol. 89, No. ST2, April 1963, p. 161.*
5. Chen, W. F. General Solution of Inelastic Beam-Column Problem *Journal of the Engineering Mechanics Division, ASCE, Vol. 96, No. EM4, August 1970, pp. 421-441.*
6. Chen, W. F. Further Studies of an Inelastic Beam-Column Problem *Fritz Engineering Laboratory Report No. 331.6, January 1970.*
7. Chen, W. F. and Santathadaporn, S. Review of Column Behaviour under Biaxial Loading *Journal of the Structural Division, ASCE, Vol. 94, No. ST12, December 1968, pp. 2999-3021.*
8. Culver, C. G. Exact Solution of the Biaxial Bending Equations *Journal of the Structural Division, ASCE, Vol. 92, No. ST2, April 1966, pp. 63-83.*
9. Ellis, J. S., Jury, E. J., and Kirk, D. W. Ultimate Capacity of Steel Columns Loaded Biaxially *E.I.C.-64-BR and STR2, Transactions of the Engineering Institute of Canada, Vol. 7, No. A-2, February 1964.*

10. Galambos, T. V. Review of Tests on Biaxially Loaded Steel Wide-Flange Beam-Columns *Fritz Engineering Laboratory Report No. 287.4, April 1963.*
11. Johnston, B. G., Ed. Guide to Design Criteria for Metal Compression Members *2nd Ed., John Wiley & Sons, Inc., New York, 1966.*
12. Lim, L. C. and Lu, L. W. The Strength and Behaviour of Laterally Unsupported Columns *Report No. 329.5, Fritz Engineering Laboratory, Lehigh University, June 1970.*
13. Marshall, P. J. and Ellis, J. S. Ultimate Biaxial Capacity of Box Steel Columns *Journal of the Structural Division, ASCE, Vol. 96, No. ST 9, September 1970, pp. 1873-1887.*
14. McDonough, J. F. The Capacity of the Biaxially Loaded Beam-Column at Ultimate Stress *Ph.D. Dissertation, University of Cincinnati, 1968.*
15. Pillai, S. U. Review of Recent Research on the Behaviour of Beam-Columns Under Biaxial Bending *Civil Engineering Research Report No. CE70-1, Royal Military College of Canada, Kingston, Canada, Jan. 1970.*
16. Ringo, B. C. Equilibrium Approach to an Ultimate Strength of a Biaxially Loaded Beam-Column *Ph.D. Dissertation, University of Michigan, Ann Arbor, Michigan.*
17. Santathandaporn, S. and Chen, W. F. Analysis of Biaxially Loaded Columns *Fritz Engineering Laboratory Report No. 331.12, September 1970.*
18. Sharma, S. S. and Gaylord, E. H. Strength of Steel Columns with Biaxially Eccentric Load *Journal of the Structural Division, ASCE, Vol. 95, ST 12, December 1969, pp. 2797-2812.*

### APPENDIX A: NOMENCLATURE AND SYMBOLS

$A_{wf}$	Total area of a wide-flange cross section
$b$	Dimension defining the position of the point of intersection of the neutral axis with the mid-line of the tension flange. The dimension is positive in the negative $x$ -direction. As a subscript, the symbol denotes specific reference to the base section.
$b_f$	Width of the flange
$d$	Dimension defining the position of the point of intersection of the neutral axis with the mid-line of the web. The dimension is positive in the positive $y$ -direction
$d_{wf}$	Depth of the wide-flange cross section measured between mid-lines of the flanges
$dM^x$ and $dM^y$	Correction terms for value of the cross section plastic moments
$e_x$	Eccentricity of the compressive force $P$ measured parallel to the $x$ -axis
$e_y$	Eccentricity of the compressive force $P$ measured parallel to the $y$ -axis
$F_y$	Yield point of material in tension and compression
$g$	General representation of proportionality constants

$M^x$	Internal moment capacity with respect to the $x$ -axis	$P_y$	The load corresponding to a cross section fully yielded under compressive stresses
$M^y$	Internal moment capacity with respect to the $y$ -axis	$t_f$	Thickness of the flange of the cross section
$M_p^x$	Full plastic moment capacity of the cross section acting about the $x$ -axis	$t_w$	Thickness of the web of the cross section
$M_p^y$	Full plastic moment capacity of the cross section acting about the $y$ -axis	$R_1$	Geometrical ratio of the thrust on a section to the thrust on the base section
$NA$	Neutral axis	$R_2$	Geometrical ratio of the moment $M^x$ on a section to the moment $M^x_b$ on the base section
$P$	Ultimate load-carrying capacity	$R_3$	Geometrical ratio of the moment $M^y$ on a section to the moment $M^y_b$ on the base section

**APPENDIX B: GROUP DESIGN GRAPHS**

W Section	Group	1/R <sub>1</sub>	W Section	Group	1/R <sub>1</sub>	W Section	Group	1/R <sub>1</sub>
W8×17	7	0.305	W12×50	6	0.720	W14×103	1	1.089
W8×20	7	0.375	W12×53	4	1.000	W14×111	1	1.173
W8×24	4	0.449	W12×58	3	1.853	W14×119	1	1.263
W8×28	4	0.526	W12×65	3	2.099	W14×127	1	1.348
W8×31	3	1.000	W12×72	3	2.332	W14×136	1	1.440
W8×35	2	1.000	W12×79	3	2.567	W14×142	1	1.514
W8×40	3	1.301	W12×85	2	2.435	W14×150	1	1.609
W8×48	1	0.510	W12×92	3	3.004	W14×158	1	1.698
W8×58	3	1.918	W12×99	3	3.241	W14×167	1	1.789
W8×67	5	1.000	W12×106	3	3.481	W14×176	1	1.887
W10×33	6	0.536	W12×120	3	3.934	W14×184	1	1.983
W10×39	4	0.732	W12×133	2	3.862	W14×193	1	2.076
W10×45	4	0.861	W12×161	5	2.405	W14×202	2	5.982
W10×49	1	0.513	W12×190	5	2.845	W14×211	2	6.241
W10×54	1	0.570	W14×43	7	0.796	W14×219	2	6.491
W10×60	1	0.632	W14×48	7	0.898	W14×228	2	6.768
W10×66	2	1.913	W14×53	7	1.000	W14×237	2	7.028
W10×72	3	2.372	W14×61	6	1.000	W14×246	2	7.306
W10×77	2	2.236	W14×68	6	1.121	W14×264	2	7.848
W10×89	2	2.591	W14×74	6	1.226	W14×287	5	4.366
W10×100	2	2.923	W14×78	4	1.496	W14×314	5	4.794
W10×112	5	1.681	W14×84	3	2.700	W14×342	5	5.224
W12×40	6	0.642	W14×87	1	0.917	W14×370	5	5.664
W12×45	6	0.720	W14×95	1	1.000	W14×398	5	6.100
						W14×426	5	6.549